

UPWIND TERRAIN AND TEMPERATURE EFFECTS ON LENGTH SCALES OF WINDS PASSING OVER HIGH ROUGHNESS (SITKA SPRUCE) WITH ESDU COMPARISONS

A.J.G. PAPESCH¹ and B.A. GARDINER²

¹Mechanical Engineering Dept, University of Canterbury, Christchurch, NEW ZEALAND

²British Forestry Commission, Roslin, Scotland, UNITED KINGDOM

ABSTRACT

Wind damage in forest plantations can be understood by measuring wind effects near mean forest height in full scale and wind tunnel models. Critical measurements are the size, speed and number, or "length scale", of eddies at forest mean height. Forest geometry, especially wider tree spacings, enhance turbulent eddies to interact with the trees. As a result, tree sway motions cause above ground stem fracture or the trees up-root and topple.

Turbulence length scales were measured just above a Sitka Spruce forest in Scotland. Orthogonal arrays of Sonic, Gill and Lowne vane anemometers were positioned up a 30m mast. Data were collected from winds from the southwest (no upwind obstruction) and west-northwest (upwind hill obstruction). The length scales were graphed and compared with ESDU standards 74031 and 85020 used to scale winds over high roughness. Along-wind length scales were the same as ESDU 85020. At 2H, across-wind and vertical length scales were all similar. At the test site, length scales were changed by the presence of a hill 1 Km upwind. It seems that large vortices shed from the hill are disturbed by the forest surface roughness, adding smaller eddies to wind energy spectra. The length scales of these eddies near canopy height H, suggest that vortices amplify wind speed and direction change while coriolis force (in ESDU 85020) has little effect. Air stability and mean wind speeds had a slight effect on length scales.

It appears that ESDU 85020 formulae, need further refinement to accurately represent across-wind and vertical length scales over high roughness. The formulae neglect vortex terms which appear in the general Navier Stokes boundary layer equations.

NOTATION

d = zero plane displacement
f = $2 \Omega \sin \phi$ = coriolis force
h = boundary layer gradient height = $u_p^*/6f$
h = hill height
H = mean forest or tree height
Hz = wind frequency in hertz
 K_z = Kolmogorov constant
 L_u = along-wind turbulence length scale
 L_v = across-wind turbulence length scale
 L_w = vertical turbulence length scale
R = adjusted regression coefficient
 Ri_g = gradient Richardson number
S = mean tree spacing within forest
 T° = mean along-wind direction, degrees true
U = mean wind speed
 u_p^* = profile friction velocity
x = along-wind direction
y = across-wind direction
z = vertical height above ground
z = height above d, = (z-d)
 z_c = height to where K_z is constant
 z_o = aerodynamic roughness
 σ_u = along-wind rms turbulence
 Ω = angular velocity of earth
 ϕ = local angle of latitude
 ϕ_c = ratio of buoyant to dissipative energy

INTRODUCTION

In man-made forests, wider tree spacings aid stem volume increment. But high spacing allows eddies to penetrate the canopy increasing tree-top movement. This adjusts the size, speed and number, or length scale of eddies. If tree sway at fundamental frequencies interacts with the eddies at tree-top height, then these eddies must break up further downwind interacting with the downwind tree crowns. This can amplify tree sway motions and overload tree stems and root systems.

Physical systems, like forests and shelterbelts, are tested in wind tunnels with winds modelled to ESDU standards (Papesch 1985, 1991). The ESDU wind structure had the full spectra of wind eddies and therefore length scales, in the along-wind direction. For high roughness, ESDU 85020 (supersedes ESDU 74031) has coriolis force, friction velocity and turbulence terms varying with height. ESDU 74031 had only d and z_o roughness terms.

Wind data from anemometers up a mast were collected over a Sitka Spruce forest in Rivox, Scotland. The length scales measured in all three orthogonal directions were calculated, graphed and compared with ESDU formulae. The Rivox regressions, below each graph in the Appendix, will help ESDU 85020 modifications.

PREVIOUS RESEARCH AND ESDU STANDARDS

Length scales over smooth terrain are now accurately represented by ESDU standards because ample full scale measurements were available for analysis. Over larger roughness, spectra measured over wheat, maize and rice, and also forests are not common and data are more widely scattered. Earlier research showed that by careful choice of axes, wind spectra (and hence length scales) collapsed on to one curve. Normalized data using ϕ_c in the denominator of the vertical axis of spectra curves reduced data scatter. Low frequency scatter remained and Ri_g dependence was not clear.

For high roughness, the later ESDU 85020 formulae should be more accurate than ESDU 74031. Since roughness alters as forest geometry is changed by tree spacing or the wind itself, z_o is not constant and length scales near the roughness vary. ESDU admit errors as high as $\pm 30\%$ in these formulae when turbulence becomes anisotropic. ESDU 85020 notes that scales over rough terrain, are not accurate as no reliable measurements exist for strong winds: L_v and L_w in strong winds "are likely to be of the same order as for L_u " [not the case in this work].

ESDU 74031 formulae for x , y , and z directions are :-

$$L_u = 25 (z^{0.35}/z_0^{0.063}) \text{ meters, (i)}$$

$$L_v = 5.1 (z^{0.48}/z_0^{0.086}) \text{ meters, (ii)}$$

and $L_w = 0.35 z \text{ meters. (iii)}$

In equilibrium winds greater than 10m/s and up to 300m (at z_c) above the ground, ESDU 85020 formulae for these same conditions are :-

$$L_u = \frac{A^{2/3}(\sigma_u/u_p^*)^3 z}{2.5 K_z^{3/2} (1-(z/h))^2 (1+5.75z/h)} \text{ (iv)}$$

$$L_v = L_u \cdot 0.5 (\sigma_v/\sigma_u)^3 \text{ (v)}$$

and $L_w = L_u \cdot 0.5 (\sigma_w/\sigma_u)^3 \text{ (vi)}$

Near the ground, $A = 0.142[1 + 0.315(1 - z/h)^6]^{2/3}$

ESDU introduced A to reduce differences between length scales derived from spectral curves (often larger) and from autocorrelation functions. ESDU 85020 give $K_z = K_w = 0.188$ above height, z_c [from 159m to 287m in this work]. Below z_c , the modified K_z calculations completely distorted along-wind length scales derived from ESDU 85020 making them excessively small. Although winds near the canopy are not fully isotropic, $K_z = 0.15$ gave excellent agreement between ESDU 85020 and Rivot along-wind length scales.

TEST SITE, INSTRUMENTS AND MEASUREMENTS

The experimental site was at Rivot (55° 19.5'N, 3°33'W), near Moffatt in South-west Scotland. The site, at 360m elevation within a broad valley basin, is gently sloping ($\approx 3^\circ$) in the direction of the prevailing south-west wind. 9.2 hill heights up-wind and west of north-west, Hangingshaw Hill (aspect ratio ≈ 3) rises a further 109m. The hill's rounded shape complicates the airflow (Inglis et.al., 1991).

The Sitka Spruce forest ($H = 15m$) was planted in 1962 at 3584 stems/ha ($S/H = 0.11$). A 30 metre 100mm diameter tubular mast fixed to a shorter tower near a local automatic weather station protruded through the canopy. 4 Sonic and 3 Gill triaxial anemometers were spaced up the mast above the canopy. 1 Gill and 4 Leda (mica-vaned) triaxial anemometers were mounted on booms to the tower within the canopy but their data was not used. All instruments have small distance constants with good accuracies and resolutions (Scannell 1984, Papesch 1985). They were calibrated before and after the field programme and a number of comparisons made with different anemometer types close together at canopy height. Temperatures were derived from 3 Sonic anemometers; the speed of sound and temperature are related. 1 hour data collection periods extended from March 1988 to January 1989 and concentrated on neutral windy days. Mean and turbulent wind profiles with a brief account of the wind skewness and structure are given by Gardiner, 1991: at canopy height H , $L_u \approx H$ and $L_w \approx H/3$.

All signals were passed through an A/D converter and recorded on 1/2" magnetic tape or a PC computer. The sonic data were recorded unfiltered at 40 Hz, twice their update frequency. All other signals were low-pass filtered and sampled at 10Hz. Initial data analysis of each tape removed wild points and found mean wind speeds. Data were then mathematically rotated to point along-wind, across-wind and vertically with compensation for the 3° terrain slope.

To avoid truncation of total variance estimates, 10 minute data samples were taken off the magnetic tapes. To inhibit Nyquist foldback, sampling rate was at over twice the highest wind frequency. Since errors increase as turbulence intensities rise above 30%, data sets chosen had high mean wind speeds. 5 data sets were used for auto-correlation length scales for each mean wind speed, direction and temperature gradient. These data sets were sorted for terrain and atmospheric stability differences. Length scales from the unobstructed southwest direction and the obstructed winds off Hangingshaw Hill were compared. They were also compared with ESDU 85020 and ESDU 74031 using actual z_0 , d and u_p^* data listed in Table 1.

TABLE 1. SUMMARY OF WIND PROFILE DATA.

Tape	T°	d	z_0	u_p^*	Ri_g	Air
26	205	8.9	1.17	1.91	.242	Neutral
27a	213	9.3	1.50	2.22	.201	Neutral
49	209	10.2	.61	1.42	.191	Neutral
50	220	9.2	1.36	2.07	.189	Neutral
51a	225	9.9	.74	1.07	.158	Neutral
33	254	11.4	.42	1.05	.348	Stable
33a	254	10.4	.97	1.05	.432	Stable
39	198	10.8	.41	.62	1.060	Stable
47a	231	10.5	.84	1.01	.515	Stable
48	233	10.4	.87	1.25	.363	Stable
51	225	8.7	1.70	1.63	1.103	Stable
35	288	10.7	.62	1.13	.374	Stable
38	291	11.3	.49	.79	.656	Stable
38b	291	11.3	.49	.79	.656	Stable
40a	264	11.8	1.01	.76	.468	Stable
41	283	10.6	1.07	.72	2.548	Stable
43	310	8.5	1.88	1.13	-.119	Neutral

The following data checks were made:-

- Anemometers were continually operationally accurate
- 10 and 60 minute runs for consistent length scales
- z_0 , d and u_p^* best fits : correlations from 0.9 to 1.0
- Single tape data regressions consistent before combined
- $K_z = 0.15$, not as defined in ESDU 85020 (see above)
- $L_{(u,v,w)}$ cross-over errors and spectra peak equivalence

RESULTS OF LENGTH SCALE COMPARISONS

The mast was 9.2 hill heights (x/h) away from Hangingshaw hill top. Hansen (1975) points out that vortex wakes behind hemispherical shapes (above hill shape) exist far longer ($> x/h$ of 20) than do momentum wakes. He concluded that wake persistence behind a hemisphere was due to the presence of vortices in the combined vortex and momentum wake. Persistence behind the obstruction decreased as turbulence intensity rose in the approach flow to the obstruction. He observed a shift of spectral energy to higher frequencies in the combined lee wake. His vortex wakes had large areas of mean wind excess and turbulence intensity deficit not seen in momentum wakes.

From Figures 1 to 9, (see Appendix) unobstructed along-wind length scales were the same as ESDU 85020. Also across-wind and vertical length scales were similar to ESDU 85020 at 2H but larger at H. Off Hangingshaw hill, along-wind length scales at 2H were lower than ESDU 85020 but similar at H. Across-wind and vertical length scales were similar at 2H and but larger than ESDU 85020 at H. Vertical length scales altered slightly. At 2H, the Rivot ratios of $L_u : L_v : L_w$ were 11 : 2.9 : 1 unobstructed and 4.6 : 2.3 : 1 obstructed.

The ESDU relationships are derived from the Logarithmic Law which neglects the vortex terms in the Navier Stokes equations.

Vortices add length scales to the wind spectra an order of magnitude smaller than do coriolis effects, currently in ESDU formulae. It appears that vortex terms must be included as shear from vortices passing over the forest creates extra turbulence. Also, vortex stretching can enhance wind speed and direction changes just above the roughness. Coriolis force had little effect on calculated length scales.

For wind tunnel modelling, ESDU 85020 formulae of along-wind length scales for high roughness are satisfactory. Just above the forest canopy, vortex wakes might influence length scale calculations in the across-wind and vertical directions. Their effect may need to be included in the ESDU relationships. ESDU 74031 is satisfactory for across-wind and vertical length scale calculations.

In this work, air stability did not alter length scale calculations enough to separate differences between unstable, neutral and stable atmospheres. Unobstructed flow over the canopy suggests that stable air might induce higher length scales but this need further investigation.

Measured mean aerodynamic roughness, z_0 near 0.1H, and displacement height, d near 1m are similar to earlier research measurements for high roughness.

CONCLUSIONS

The along-wind length scale measurements compare well with ESDU standard 85020. Across-wind and vertical length scales were similar to ESDU 85020 at 2H but larger at H. Behind the hill, along-wind and across-wind length scales might be influenced by the combined momentum and vortex wake conditions observed by Hansen in wind tunnel tests. Vertical length scales were unchanged. Length scales were less dependent on atmospheric stability or mean winds.

It appears that ESDU 85020 needs further refinement to predict more accurately length scales near high roughness.

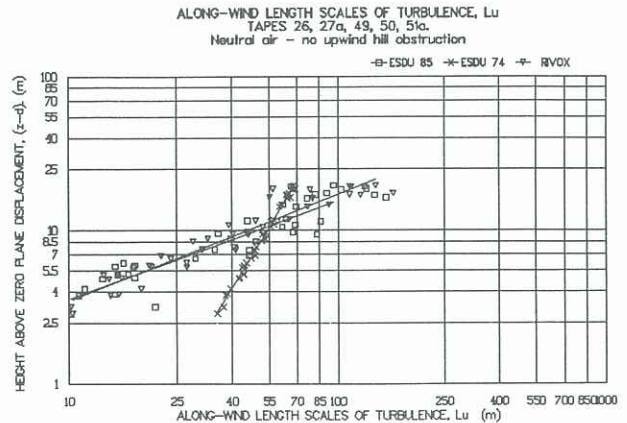
ACKNOWLEDGEMENTS

The authors thank the British Forestry Commission, the University of Canterbury and the British High Commission in New Zealand for travel and financial support.

REFERENCE LIST

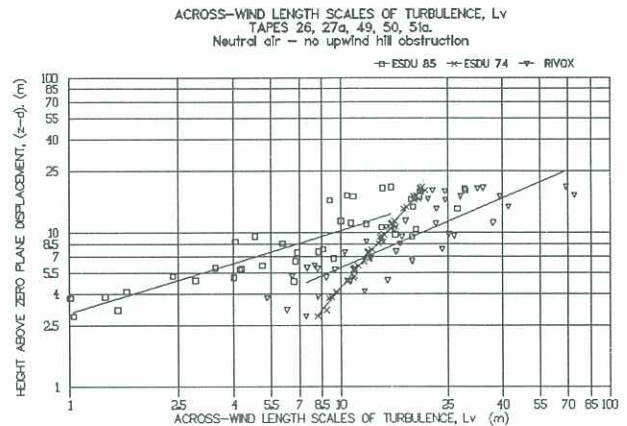
- ARYA P(1988) An Introduction to micro-meteorology. Acad.Press 307p.
- ENGINEERING SCIENCES DATA UNIT (1974) Characteristics of atmospheric turbulence near the ground, Part II, ESDU 74031.
- ENGINEERING SCIENCES DATA UNIT (1985). Characteristics of atmospheric turbulence near the ground, Part II, ESDU 85020.
- INGLIS, D W F, GARDINER, B A, and CHOULARTON, T W (1991) A model of airflow above and within a forest canopy in a region of complex terrain. 20th Agric. & Forest Met. Conference. Utah, USA. 4p.
- GARDINER, B A (1991) Observations of airflow above and within conifer plantations. 20th Agric. & Forest Met. Conference. Utah, USA. 4p.
- HANSEN, A C (1975) Vortex-containing wakes of surface obstacles. PhD. Colarado University, Fort Collins, USA. 163p.
- HAUGEN, D A (1973) Editor. Workshop on Micro-meteorology. American Meteorological Society. 392 p.
- PAPESCH, A J G (1985) Wind and its effects on Forests, PhD. University of Canterbury, New Zealand. 356p.
- PAPESCH, A J G (1991) Wind tunnel tests to optimize barrier spacing and porosity to reduce wind damage in horticultural shelter-systems. 8th World Conf. on Wind Engineering. Univ. of Western Ontario, Canada.
- PLATE, E J (1982) Editor. Engineering meteorology. Elsevier Publishing Company. 740 p.
- SCANELL, B (1984) Qualification of the Interactive Motions of the Surface Layer and a Conifer Canopy. PhD. Cranfield Inst. of Tech., UK.
- STULL, R B (1988) An introduction to Boundary Layer Meteorology. Kluwer Academic Publishers, Holland. 666 p.
- WALMSLEY, J L et. al. (1990) Surface-layer flow in complex terrain: Comparison of models and full-scale observations. *Boundary Layer Meteorol.* 52 : 259-281.

APPENDIX - GRAPHED LENGTH SCALES.



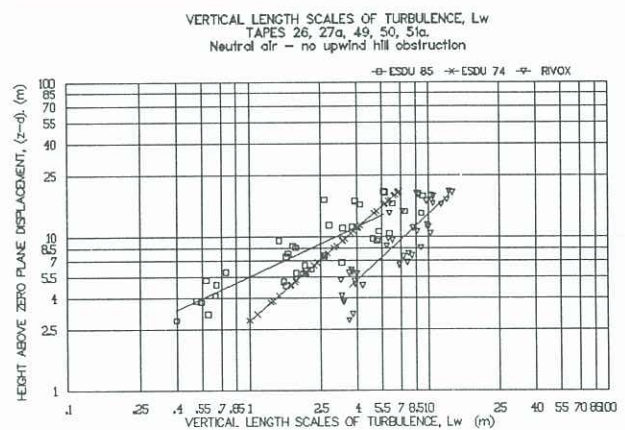
$$L_u(\text{Rivos}) = 1.55((z-d)/z_0)^{1.52} \quad (z_0 = 1.08, R^2 = 0.911)$$

FIG 1. L_u v $(z-d)$, Ri_g (.25 to -.25), No Obstruction.



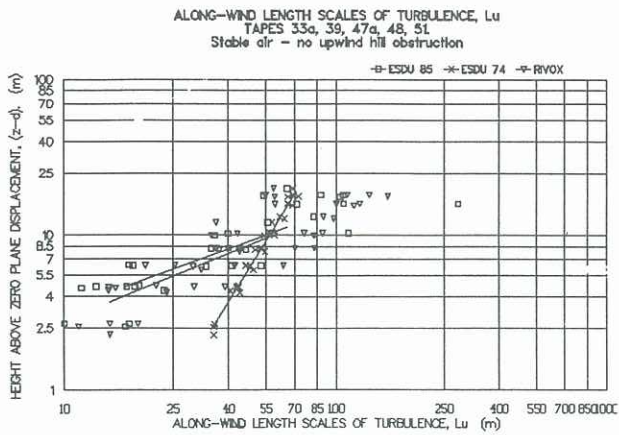
$$L_v(\text{Rivos}) = 1.00((z-d)/z_0)^{1.35} \quad (z_0 = 1.08\text{m}, R^2 = 0.720)$$

FIG 2. L_v v $(z-d)$, Ri_g (.25 to -.25), No Obstruction.



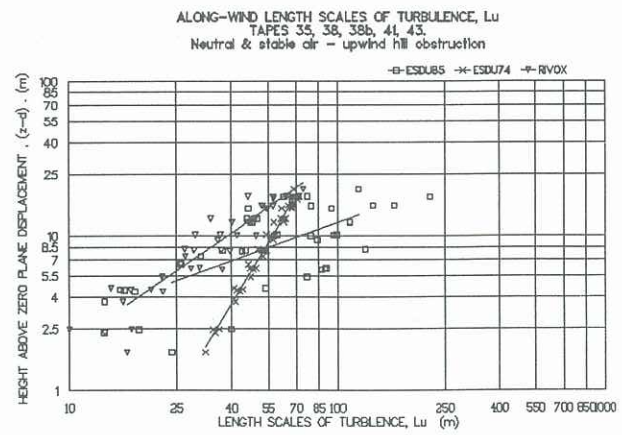
$$L_w(\text{Rivos}) = 1.01((z-d)/z_0)^{0.94} \quad (z_0 = 1.08\text{m}, R^2 = 0.763)$$

FIG 3. L_w v $(z-d)$, Ri_g (.25 to -.25), No Obstruction



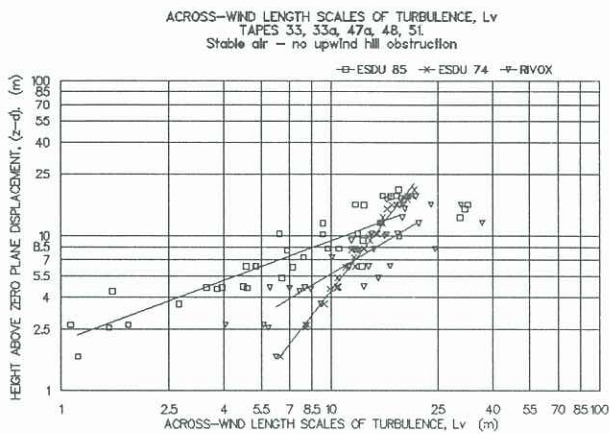
$$L_u(\text{Rivox}) = 1.65((z-d)/z_0)^{1.38} \quad (z_0 = 0.87, R^2 = 0.725)$$

FIG 4. L_u v $(z-d)$, R_i above 0.25, No Obstruction



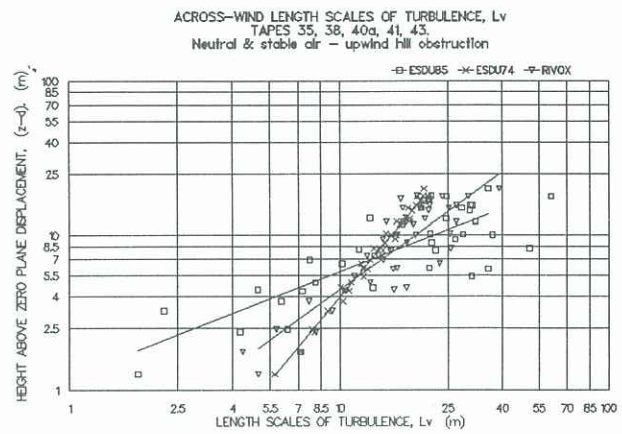
$$L_u(\text{Rivox}) = 6.13((z-d)/z_0)^{0.87} \quad (z_0 = 0.97\text{m}, R^2 = 0.859)$$

FIG 7. L_u v $(z-d)$, R_i > -0.25, Hill Obstruction



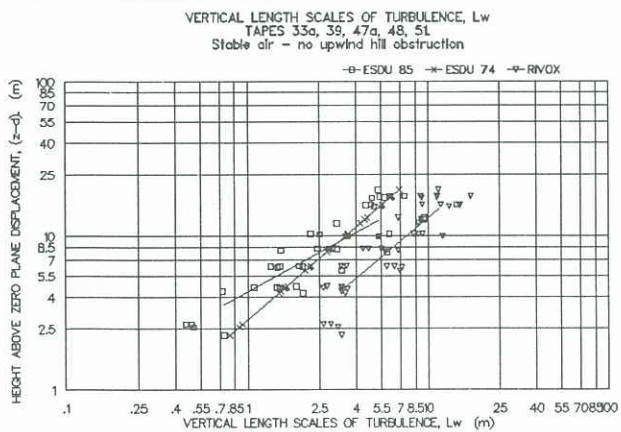
$$L_v(\text{Rivox}) = 2.00((z-d)/z_0)^{0.87} \quad (z_0 = 0.87, R^2 = 0.764)$$

FIG 5. L_v v $(z-d)$, R_i above 0.25, No Obstruction



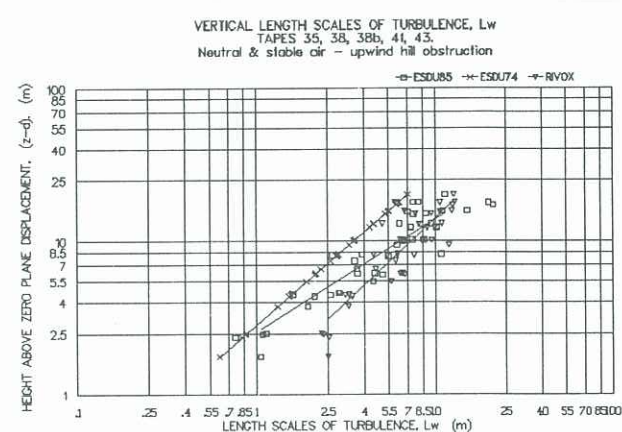
$$L_v(\text{Rivox}) = 3.73((z-d)/z_0)^{0.79} \quad (z_0 = 0.97\text{m}, R^2 = 0.748)$$

FIG 8. L_v v $(z-d)$, R_i > -0.25, Hill Obstruction



$$L_w(\text{Rivox}) = 0.64((z-d)/z_0)^{1.02} \quad (z_0 = 0.87, R^2 = 0.777)$$

FIG 6. L_w v $(z-d)$, R_i above 0.25, No Obstruction



$$L_w(\text{Rivox}) = 1.18((z-d)/z_0)^{0.81} \quad (z_0 = 0.97\text{m}, R^2 = 0.783)$$

FIG 9. L_w v $(z-d)$, R_i > -0.25, Hill Obstruction